Posttranslational myristoylation of caspase-activated p21-activated protein kinase 2 (PAK2) potentiates late apoptotic events

Gonzalo L. Vilas, Maria M. Corvi*, Greg J. Plummer*, Andrea M. Seime, Gareth R. Lambkin, and Luc G. Berthiaume†

Department of Cell Biology, Faculty of Medicine and Dentistry, University of Alberta, Edmonton, AB, Canada T6G 2H7

Edited by Jeffrey I. Gordon, Washington University School of Medicine, St. Louis, MO, and approved March 8, 2006 (received for review February 3, 2006)

p21-activated protein kinase (PAK) 2 is a small GTPase-activated serine/threonine kinase regulating various cytoskeletal functions and is cleaved by caspase-3 during apoptosis. We demonstrate that the caspase-cleaved PAK2 C-terminal kinase fragment (C-t-PAK2) is posttranslationally myristoylated, although myristoylation is typically a cotranslational process. Myristoylation and an adjacent polybasic domain of C-t-PAK2 are sufficient to redirect EGFP from the cytosol to membrane ruffles and internal membranes. Membrane localization and the ability of C-t-PAK2 to induce cell death are significantly reduced when myristoylation is abolished. In addition, the proper myristoylation-dependent membrane localization of C-t-PAK2 significantly increased signaling through the stress-activated c-Jun N-terminal kinase signaling pathway, which often regulates apoptosis. Interestingly, C-t-PAK2 promoted cell death without compromising mitochondrial integrity. Posttranslational myristoylation of caspase-cleaved proteins involved in cytoskeletal dynamics (e.g., PAK2, actin, and gelsolin) might be part of a unique series of mechanisms involved in the regulation of the later events of apoptosis.

apoptosis | cytoskeleton | mitochondria | membrane | acylation

Apoptosis, or programmed cell death, is a fundamental process in the development of multicellular organisms. Apoptosis enables an organism to eliminate unwanted or defective cells through an organized process of cellular disintegration that has the advantage of not inducing an inflammatory response (1). Improper regulation of apoptosis occurs in disorders such as cancer, viral infection, autoimmune disease, and neurodegenerative disorders (2, 3). Although apoptosis is initiated by many physiological and pathological stimuli, all apoptotic cells undergo a similar sequence of morphological changes, including membrane blebbing, cell shrinkage, nuclear and cytoplasmic condensation, and, finally, fragmentation into apoptotic bodies (4).

Two distinct but interconnected apoptotic pathways regulate cell death, the extrinsic or receptor-mediated pathway and the intrinsic or mitochondrial pathway (5, 6). Both pathways result in the activation of a variety of caspases (7). Upon binding of ligands (e.g., Fas/CD95 ligand) to their respective receptors, the receptors trimerize, recruit Fas-associated death domain protein, and activate the initiator caspase-8. Caspase-8 then activates executioner caspases (e.g., caspase-3, -6, and -7) (5). A variety of extracellular cues and intracellular insults such as serum withdrawal or DNA damage activate the intrinsic or mitochondrial pathways. These stresses lead to loss of mitochondrial membrane potential ($\Delta_{\Psi m}$), release of proteins (e.g., cytochrome *c* and apoptosis inducing factor), activation of caspase-9, and formation of the apoptosome, which further promotes cleavage and activation of executioner caspase-3 (1). Among the targets of executioner caspases are many cytoskeletal proteins (actin, gelsolin, and focal adhesion kinase) and proteins involved in cell signaling, apoptosis regulation, and DNA repair. By cleaving these proteins, it is believed that caspases turn off cell survival and turn on cell disassembly.

During apoptosis, caspase-8-cleaved Bid (a Bcl-2 family member) is posttranslationally myristoylated before relocalization to mitochondria (8). Typically, *N*-myristoylation is a cotranslational process. In *N*-myristoylation, the 14-carbon fatty acid myristate is added to an essential N-terminal glycine residue by means of an amide bond after the removal of the initiator methionine residue. The consensus sequence recognized by *N*-myristoyl transferase (NMT) is M-G-X-X-X-S/T/C, with, preferentially, a lysine or arginine residue at positions 7 and/or 8 (9, 10). By itself, a myristoyl moiety added to a protein is not sufficient to confer stable membrane anchoring. Instead, an adjacent or remote second signal in the form of a polybasic stretch of amino acids or of one or two palmitoyl-cysteine residues is often required for stable membrane binding and proper membrane targeting (10, 11).

Following the original demonstration of posttranslational myristoylation of truncated Bid (myr-t-Bid) (8), posttranslational myristoylation of two caspase-cleaved cytoskeletal proteins, actin and gelsolin, was demonstrated by using a recombinant expression system of short sequences fused to TNF (myr-t-actin and myr-t-gelsolin) (12). Although myr-t-actin was shown to colocalize with mitochondria, like myr-t-Bid, the role of myristoylation in the subcellular localization of myr-t-gelsolin was not investigated (12).

p21-activated protein kinase (PAK) 2 is a serine/threonine kinase activated by the small GTPases CDC42 and Rac (13) and is involved in the regulation of various cytoskeletal functions, including cell motility (14) and membrane blebbing during apoptosis (15). Of the six PAK family members, only PAK2 is ubiquitously expressed and cleaved by caspase-3 (14–16). This cleavage removes the 28-kDa N-terminal regulatory domain and generates a constitutively active 34-kDa PAK2 C-terminal kinase fragment (C-t-PAK2) (15). Amino acid sequence analysis adjacent to the caspase-cleavage site (7) of PAK2 (G-A-A-K-S-L-D-K-Q-K-K-K-P-K) reveals a putative internal myristoylation sequence (9, 10, 14) followed by a short stretch of basic amino acid residues often required for membrane association (9–11) (Fig. 5, which is published as supporting information on the PNAS web site).

In this study, we demonstrate that upon caspase-3 cleavage of PAK2, C-t-PAK2 is indeed posttranslationally myristoylated (myr-C-t-PAK2). myr-C-t-PAK2 is enriched in specific regions of the plasma membrane (membrane ruffles) and internal membranes, where it promotes cell death via an increased signaling through the stress-activated signaling pathway leading to c-Jun N-terminal kinase (JNK) phosphorylation. Interest-

Conflict of interest statement: No conflicts declared.

This paper was submitted directly (Track II) to the PNAS office.

Abbreviations: PAK, p21-activated protein kinase; C-t-PAK2, PAK2 C-terminal kinase fragment; JNK, c-Jun N-terminal kinase; HMA, 2-hydroxymyristic acid; NMT, *N*-myristoyl transferase; PVDF, poly(vinylidene difluoride); STS, staurosporine; GAP, growth-associated protein.

*M.M.C. and G.J.P. contributed equally to this work.

†To whom correspondence should be addressed. E-mail: luc.berthiaume@ualberta.ca.

www.pnas.org/cgi/doi/10.1073/pnas.0600824103

ingly, myr-C-t-PAK2 promoted the later events of cellular death without compromising mitochondrial integrity. Our results indicate that myr-C-t-PAK2 is a prototypical posttranslationally myristoylated caspase-cleaved protein that is involved in cellular death regulation.

Results

To determine whether C-t-PAK2 was indeed myristoylated (Fig. 5*A*), we used peptides encompassing the first 10 amino acids of C-t-PAK2 in an *in vitro* myristoylation assay, followed by MS analysis. We found that the wild-type peptide GAAKSLDKGK (Gly-213-N10-PAK2) was myristoylated in the presence of both myristoyl-CoA and NMT and presented the 1,255 m/z peak corresponding to the chemically myristoylated peptide standard (Fig. 5*B*). The nonmyristoylatable peptide where the essential glycine (Gly-213) had been substituted to alanine (Ala-213-N10-C-t-PAK2) did not show a m/z peak at 1,268, indicating that this peptide was not a substrate for NMT. Taken together, these results suggest that NMT can myristoylate the peptide encompassing the first 10 amino acids of the caspase-3-cleaved PAK2 *in vitro*.

To confirm whether C-t-PAK2 was myristoylated *in vivo*, we metabolically labeled Jurkat T cells with [^{3}H]myristate and treated them with staurosporine (STS) or left them untreated (17) for 5 h. Fluorographic analysis of the blotted proteins indicated that the immunoprecipitated endogenous 34-kDa C-t-PAK2 incorporated radiolabeled myristate (Fig. 1*A*). This result suggests that endogenous C-t-PAK2 is posttranslationally myristoylated in apoptotic Jurkat T cells.

To determine whether posttranslational myristoylation of C-t-PAK2 is catalyzed by NMT, we used the NMT inhibitor 2-hydroxymyristic acid (HMA). When incorporated into the cells, HMA is metabolically converted to 2-hydroxymyristoyl-CoA, a specific inhibitor of NMT (18) and does not inhibit protein palmitoylation (19, 20). When Jurkat T cells were cultured in the presence or absence of 1 mM HMA, metabolically labeled with [^{3}H]myristate, and induced to undergo apoptosis with STS or left untreated (Fig. 1*B*), HMA prevented [^{3}H]myristate incorporation into endogenous C-t-PAK2 but did not impair caspase-3-mediated PAK2 cleavage upon STS treatment. HMA treatment alone did not induce PAK2 cleavage in Jurkat T cells. The specific HMA inhibition further illustrates the involvement of NMT in endogenous C-t-PAK2 myristoylation.

To investigate whether C-t-PAK2 was *N*- or *S*-acylated, COS-7 cells were transfected with plasmids expressing a recombinant C-terminally myc-tagged C-t-PAK2 construct (Gly-213-C-t-PAK2-myc); nonmyristoylatable Ala-213-C-t-PAK2-myc; a dually palmitoylated chimeric protein, growth-associated protein (GAP) 43-GFP (11); or GFP. Transfected cells expressing PAK2 constructs were metabolically labeled with [^{3}H]myristate, whereas cells expressing GAP-43-GFP or GFP were labeled with [^{125}I]iodopalmitate as described in ref. 11, lysed, immunoprecipitated, and detected by Western blot on poly(vinylidene difluoride) (PVDF) membranes. The membranes were then treated with 0.2 M KOH (pH of ≈13.0), which cleaves both thioesters and oxyesters, or 1 M Tris·HCl (pH 7.0) (21, 22). Gly-213-C-t-PAK2-myc but not Ala-213-C-t-PAK2-myc incorporated [^{3}H]myristate. The label incorporated into Gly-213-C-t-PAK2-myc was resistant to alkali treatment (0.2 M KOH), which efficiently deacylated GAP-43-GFP. Neutral Tris treatment failed to deacylate either Gly-213-C-t-PAK2-myc or GAP-43-GFP (Fig. 1*C*). Because the substitution of Gly-213 by Ala in Ala-213-C-t-PAK2-myc did abrogate incorporation of [^{3}H]myristate, our results, which show that label is incorporated in an alkali-resistant fashion, indicate that [^{3}H]myristate label is linked to the N-terminal glycine residue of C-t-PAK2-myc by means of an amide bond.

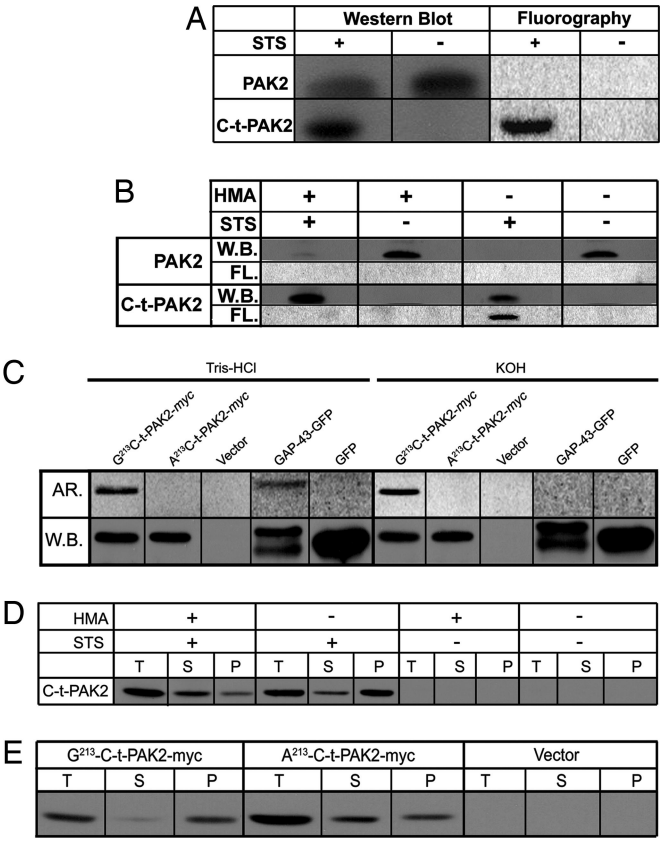

Fig. 1. C-t-PAK2 is posttranslationally myristoylated on Gly-213 by NMT during apoptosis in Jurkat T cells. (*A*) Jurkat T cells were metabolically labeled with [9,10(*n*)-^{3}H]myristate and incubated for 5 h in the absence or presence of 2.5 μM STS and 5 μg/ml cycloheximide (STS) to induce apoptosis. Cells were lysed, and PAK2 was immunoprecipitated. Immunocomplexes were analyzed by Western blotting (W.B.) and fluorography (FL). (*B*) Jurkat T cells were metabolically labeled and induced to undergo apoptosis as in *A* in the absence or presence of 1 mM HMA. Samples were analyzed as in *A*. (*C*) COS-7 cells were transfected with plasmids allowing expression of Gly-213-C-t-PAK2-myc, the nonmyristoylatable Ala-213-C-t-PAK2-myc chimeras, vector alone, a palmitoylatable (nonmyristoylated) chimeric GAP-43-GFP, or GFP. Transfected cells were metabolically labeled with [9,10(*n*)-^{3}H]myristate or [^{125}I]iodopalmitate for 4 h and lysed. Expressed proteins were immunoprecipitated and analyzed by Western blotting. PVDF membranes were then soaked for 24 h in either 0.2 M KOH or 1 M Tris·HCl (pH 7.0) and subjected to imaging with PhosphorImager screens (AR.). (*D*) Subcellular distribution of endogenous C-t-PAK2 in Jurkat T cells treated as in *B* were lysed and fractionated into total (T), cytosolic (S), and membrane (P) fractions. The presence of C-t-PAK2 was analyzed by Western blotting/enhanced chemiluminescence. (*E*) COS-7 cells were transfected with plasmids expressing Gly-213-C-t-PAK2-myc, the nonmyristoylatable Ala-213-C-t-PAK2-myc chimeras, or vector alone and were analyzed 12–14 h after transfection. Cells were subjected to subcellular fractionation and C-t-PAK2 detection as in *D*.

Posttranslationally myristoylated Gly-213 is adjacent to a short polybasic domain, a combination that is known to lead to membrane anchoring (10, 23). To investigate the role of myristoylation in the subcellular localization of C-t-PAK2, Jurkat T cells were incubated in the absence or presence of HMA, treated with or without STS for 5 h, and subjected to subcellular fractionation. In apoptotic Jurkat T cells, the vast majority of endogenous C-t-PAK2 remained soluble in the presence of the NMT inhibitor HMA (Fig. 1*D*), whereas C-t-PAK2 was found predominantly in the membrane fractions (P) in the absence of HMA. These results indicate that after caspase-3 cleavage, endogenous myristoylated C-t-PAK2 associates more efficiently with membranes.

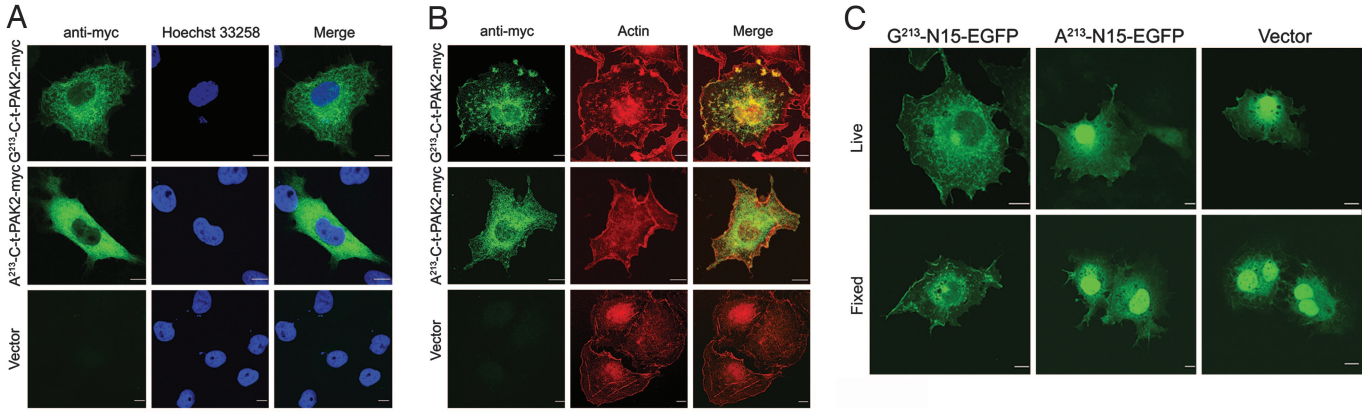

Fig. 2. Myristoylation is required for proper intracellular localization of C-t-PAK2-myc. Indirect immunofluorescence confocal micrographs of COS-7 cells transfected with plasmids allowing expression of Gly-213-C-t-PAK2-myc, the nonmyristoylatable Ala-213-C-t-PAK2-myc chimeras, or vector alone at 12–14 h after transfection. (*A*) Gly-213-C-t-PAK2-myc localizes to the plasma membrane and membrane ruffles, whereas the Ala-213-C-t-PAK2-myc chimera remains cytosolic. Shown are C-t-PAK2-myc chimeras (anti-myc, green) and nuclei (Hoechst dye 33258 staining, blue). (*B*) Confirmation of Gly-213-C-t-PAK2-myc localization to plasma membrane ruffles as indicated by colocalization with actin (red). The merged images are presented in *Right*. Yellow indicates apparent colocalization of the green and red signals. (*C*) The N-terminal 14 amino acids of C-t-PAK2 encompassing the myristoylation signal and a short polybasic domain are sufficient to localize EGFP to membranes. COS-7 cells were transfected with plasmids expressing chimeric EGFPs in which the first 14 amino acids of C-t-PAK2 (Gly-213-N15-EGFP or the corresponding nonmyristoylatable mutant Ala-213-N15-EGFP) were inserted after the initiator methionine or vector alone. Images were obtained 12–14 h after transfection. EGFP was detected either by live cell fluorescence microscopy (Live) or indirect immunofluorescence (Fixed) by confocal microscopy. (Scale bars, 10 μm.)

To assess the contribution of myristoylation to the localization of C-t-PAK2, we compared the subcellular partitioning properties of the nonmyristoylatable mutant Ala-213-C-t-PAK2-myc with those of Gly-213-C-t-PAK2-myc in transfected COS-7 cells. Fig. 1*E* shows that although the myristoylatable Gly-213-C-t-PAK2-myc was found almost exclusively in the membrane-containing fraction (P), the nonmyristoylatable Ala-213-C-t-PAK2 was found predominantly in the cytosolic fraction (S). This observation confirmed our previous findings (Fig. 1*D*) in Jurkat T cells with endogenous C-t-PAK2. In the experiments where myristoylation of C-t-PAK2 was abrogated by chemical inhibition of NMT with HMA or by site-directed mutagenesis, there was some residual C-t-PAK2 in the membrane fraction. Whether this residual membrane-associated C-t-PAK2 is due to intrinsic membrane-binding properties, impurities in the fractionation protocol, or incomplete NMT inhibition by the competitive inhibitor HMA is not known.

The subcellular localization of recombinant myristoylated or nonmyristoylated C-t-PAK2-myc was investigated next. Fig. 2*A* (and Fig. 6, which is published as supporting information on the PNAS web site) shows that Gly-213-C-t-PAK2-myc was found primarily at the plasma membrane, with apparent enrichment in membrane ruffles as judged by the extent of colocalization with the actin cytoskeletal marker TR-phalloidin (tetramethyl rhodamine-labeled phalloidin) (Fig. 2*B*). Interestingly, the actin staining pattern appeared different in cells expressing Gly-213-C-t-PAK2-myc, Ala-213-C-t-PAK2-myc, or vector alone. Actin-rich membrane ruffles were found predominantly in cells transfected with Gly-213-C-t-PAK2-myc. Cells expressing Gly-213-C-t-PAK2-myc or Ala-213-C-t-PAK2-myc were also typically devoid of stress fibers spanning the cytosol (Fig. 2*B*). The nonmyristoylatable Ala-213-C-t-PAK2-myc appeared diffuse and completely cytosolic (Fig. 2*A*). Contrasting with the nuclear localization of N-terminally tagged GFP-PAK2 constructs reported by Koeppel *et al.* (24) and Jakobi *et al.* (16), both of our C-t-PAK2-myc chimeras were excluded from the nucleus (Fig. 2*A*). These results suggest that myristoylation of C-t-PAK2 is important for proper cellular membrane localization and may stimulate membrane ruffle formation and cytoskeletal reorganization. The striking difference in localization patterns of myristoylated and nonmyristoylated C-t-PAK2-myc also suggests that the myristoylation efficiency of these proteins is likely very high if not complete.

To test whether the combination of myristate and polybasic domain found at the N terminus of C-t-PAK2 was sufficient for targeting C-t-PAK2 to membranes, the first 14 amino acids of C-t-PAK2 (G-A-A-K-S-L-D-K-Q-K-K-K-P-K) were appended at the N terminus of EGFP (Gly-213-N15-EGFP). In addition, the nonmyristoylatable version, Ala-213-N15-EGFP, was also engineered. In both fixed and live transfected COS-7 cells, the myristoylated Gly-213-N15-EGFP was excluded from the nucleus and localized to the plasma membrane, membrane ruffles, and perinuclear vesicular structures in a pattern highly similar to that of myristoylated C-t-PAK2-myc (Fig. 2*C*). In contrast, the nonmyristoylated Ala-213-N15-EGFP was found, like EGFP, partly in the cytosol but almost exclusively in the nuclei (Fig. 2*C*). These results indicate that the first 14 amino acids of C-t-PAK2 containing the myristoylation consensus sequence and a short polybasic domain are sufficient to localize EGFP to the plasma membrane, membrane ruffles, and internal structures. This localization pattern is lost when the myristoylation consensus sequence is abrogated. This finding confirms that myristoylation is required for proper membrane association and subcellular localization of C-t-PAK2. In addition, the myristoylation efficiency of the Gly-213-N15-EGFP construct is likely very high if not complete, as judged by its drastic difference in subcellular localization in comparison with Ala-213-N15-EGFP.

Caspase-3-mediated cleavage of PAK2 has been observed during apoptosis (15, 25, 26), and overexpression of the N-terminally tagged C-terminal cleavage product C-t-PAK2 has been shown to induce cell death (16, 24, 27). However, all these previous studies assessed the apoptotic activity of the nonphysiologically relevant, nonmyristoylated form of C-t-PAK2. To study the physiological form of C-t-PAK2 and assess the importance of posttranslational myristoylation of C-t-PAK2 in its ability to induce apoptosis, we compared the apoptotic properties of Gly-213-C-t-PAK2-myc and Ala-213-C by using an established EGFP cotransfection assay (16, 24, 27). Because the expression of C-t-PAK2 leads to nuclear condensation, adherent cell shrinking, and rounding up without exhibiting some of the

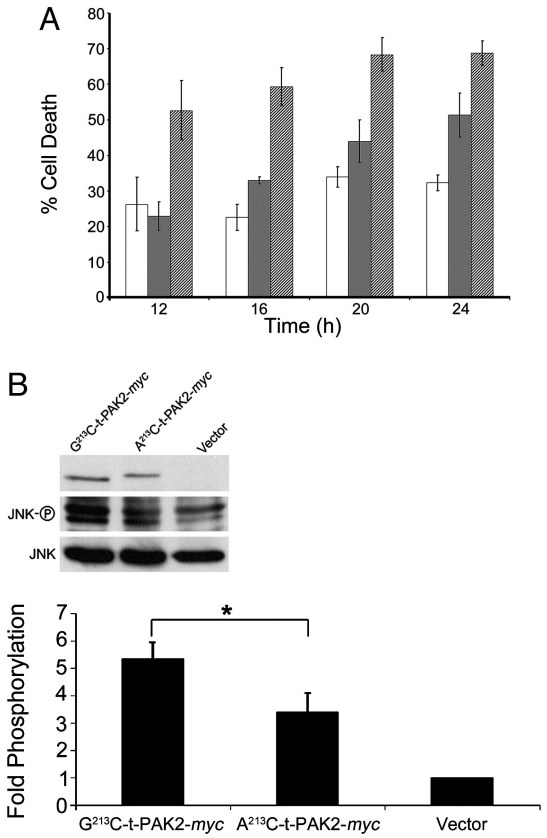

Fig. 3. Myristoylation enhances the morphological apoptotic effects of C-t-PAK2 and signaling through JNK. (*A*) COS-7 cells were cotransfected with plasmids expressing EGFP and plasmids expressing Gly-213-C-t-PAK2-myc (hatched bars), Ala-213-C-t-PAK2-myc chimeras (gray bars), or vector alone (open bars). At the indicated times, the percentage of cotransfected apoptotic cells for each time point was calculated as described in *Materials and Methods* and plotted. Data are means ± SE from three independent experiments. (*B*) Expression of C-t-PAK2 induces JNK phosphorylation. COS-7 cells were transfected with Gly-213-C-t-PAK2-myc, Ala-213-C-t-PAK2-myc chimeras, or vector alone; 14–16 h after transfection, cell lysates were made and total JNK, phospho-JNK, and myc were electroblotted and immunodetected with the proper antibodies. The intensity of the bands was determined by densitometry. Data in the histogram are presented as fold phosphorylation over vector normalized by the corresponding total JNK and C-t-PAK2-myc expression. Data represent the means ± SE of three individual experiments. *, $P \leq 0.05$.

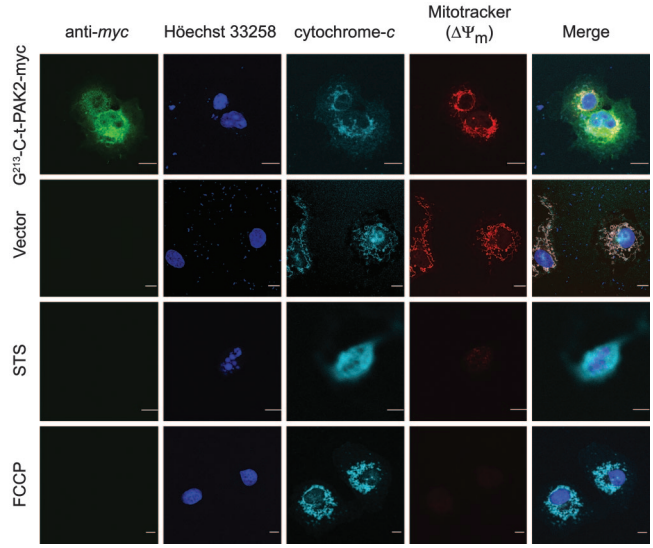

Fig. 4. C-t-PAK2 expression induces mitochondrial-independent cell death. COS-7 cells were mock-transfected or transfected with either vector expressing Gly-213-C-t-PAK2-myc or vector alone. At 16 h after transfection, cells were treated with 1 μM STS for 4 h or 5 μM *para*-trifluoromethoxy carbonyl cyanide phenylhydrazone for 15 min or left untreated. Cells were then incubated in the presence of the potentiometric dye MitoTracker red CM-H_2XRos for 30 min. After incubation, cells were processed for confocal immunofluorescence microscopy to detect C-t-PAK2-myc (green), cytochrome *c* (light blue), nuclei (blue), and mitochondrial membrane potential (red). The merged images are presented in the far-right column. (Scale bars, 10 μm.)

classical hallmarks of apoptosis (no phosphatidylserine externalization and absence of TUNEL reactivity) (27, 28), the percentage of cells undergoing apoptosis/cell death at different times after cotransfection was calculated as the percentage of green cells presenting condensed/fragmented nuclei and rounded/retracted/highly refractive morphology as described by Lee *et al.* (27), Jakobi *et al.* (16), and Koeppel *et al.* (24). Expression of the myristoylatable Gly-213-C-t-PAK2-myc chimera resulted in a count of 52% apoptotic cells after 12 h, and this amount reached a maximal plateau at ≈68% within 20 h after transfection (Fig. 3). In contrast, expression of Ala-213-C-t-PAK2-myc resulted in a significant delay in the onset of apoptotic cell death. Indeed, at the 12-h time point, cell death rate of cells expressing nonmyristoylated C-t-PAK2 is equivalent to that of vector transfected cells (≈23%) and reached ≈50% only at 24 h after transfection. Cells cotransfected with empty vector and vector expressing EGFP presented apoptotic cell death rates varying from ≈20% to 35% between early and late time points, respectively (Fig. 3*A*; see also Fig. 7, which is published as supporting information on the PNAS web site), presumably because of the reported mild toxicity of EGFP (29). These results indicate that expression of the physiologically relevant myristoylated C-t-PAK2 induces apoptotic cell death more potently than nonmyristoylated C-t-PAK2 in COS-7 cells, suggesting a key role for posttranslational myristoylation in proper localization of C-t-PAK2, cell signaling, and the regulation of cell death.

Because C-t-PAK2 was previously shown to increase JNK phosphorylation, we then compared the ability of myristoylatable and nonmyristoylatable C-t-PAK2-myc to induce the stress-activated pathway leading to JNK activation. At 14–16 h after transfection, COS-7 cells transfected with Gly-213-C-t-PAK2-myc resulted in a >5-fold increase in JNK phosphorylation when compared with vector transfected cells. In contrast, JNK phosphorylation of Ala-213-C-t-PAK2-myc transfected cells was only ≈3.5-fold (Fig. 3*B*). The overall 1.5-fold increased stimulation of JNK phosphorylation by the myristoylated C-t-PAK2 over the nonmyristoylated C-t-PAK2 was statistically significant ($n = 4$; $P \leq 0.05$ in a Student *t* test). These results indicate that myristoylated C-t-PAK2 is again more effective than nonmyristoylated C-t-PAK2. Interestingly, the slower electrophoretic mobility of Ala-213-C-t-PAK2-myc observed in Fig. 2*B* was highly reproducible and was shown to be caused by an increased phosphorylation of the protein, because treatment of immunoprecipitated Ala-213-C-t-PAK2-myc with alkaline phosphatase abolished such migration difference (data not shown). Therefore, it appears that proper myristoylation of C-t-PAK2 might also relocalize it away from the effects of an unidentified cytosolic kinase.

To assess the involvement of mitochondria in the death process, we investigated the cytochrome *c* release and loss of mitochondrial potential in transfected COS-7 cells. At 16 h after transfection, cells expressing G-213-C-t-PAK2-myc undergoing apoptosis (as judged by nuclear condensation and cellular retraction) did not release cytochrome *c* into the cytosol and did not lose their mitochondrial potential as assessed by indirect immunofluorescence and the potentiometric dye MitoTracker

red CM-H_2XRos (30) (Fig. 4). Similar results were observed in cells expressing the nonmyristoylatable Ala-213-C-t-PAK2-myc chimera (data not shown). In contrast, COS-7 cells treated with STS readily released cytochrome *c*, and cells treated with the uncoupling reagent *para*-trifluoromethoxy carbonyl cyanide phenylhydrazone readily lost their mitochondrial potential. These results suggest that the later apoptotic events stimulated by myr-C-t-PAK2 (nuclear condensation, cell retraction, and rounding up leading to detachment) occur downstream of the mitochondrial apoptosis commitment step and indicate that these C-t-PAK2-dependent morphological changes do not activate the intrinsic apoptotic pathway.

Discussion

PAK2 is the only PAK cleaved by caspases in the later events of apoptosis (14). Although myristoylation is typically a cotranslational process, we demonstrate that caspase-activated C-t-PAK2 is enzymatically posttranslationally myristoylated by NMT. Myristoylation of C-t-PAK2 redirected it to the plasma membrane and membrane ruffles, where it promoted cell death via an increased signaling through JNK but without compromising mitochondrial integrity. The relocalization and enrichment of myristoylated C-t-PAK2 in plasma membrane and membrane ruffles upon posttranslational myristoylation is previously undocumented and contrasts with the previous localizations of myr-t-Bid and myr-t-actin, which were both found on mitochondria (8, 12). When appended to the EGFP reporter protein, the N-terminal 14 amino acids of C-t-PAK2 encompassing the myristoylation signal and a short polybasic domain were shown to be sufficient to confer a subcellular localization highly similar to that of the entire myristoylated C-t-PAK2 protein. These results corroborate our previous results and those of others that suggest that various short N-terminal domains encoding for combinations of myristoylation and polybasic signals or myristoylation and palmitoylation signals are plasma membrane targeting signals (10, 11, 23).

Caspase-3 cleavage removes most of the known protein–protein interacting domains found in PAK2. Interestingly, the membrane-bound small GTPase Rac, a PAK2 activator, (14) was recently shown to be caspase-cleaved and inactivated during apoptosis (31). Therefore, removal of the PAK2 inhibitory domain in conjunction to proper myristoylation might serve not only to activate the PAK2 kinase domain independent of small GTPases but also to relocate the kinase domain toward membrane regions of the cell enriched in PAK2 substrates such as myosin light chain kinase, myosin heavy chain/myosin light chain, and LIM kinase (14). This activation/relocation step could lead, in part, to a better activation of the stress-activated signaling pathway as seen by the increased JNK phosphorylation (Fig. 3) and argues in favor of a stress signaling pathway that originates at membranes. In addition, cells expressing myr-C-t-PAK2 also presented significant alterations in their cytoskeleton and exhibited a significant increase in the number of membrane ruffles and apparent loss of stress fibers (Fig. 3). As such, proper myristoylation of C-t-PAK2 made it better at promoting cytoskeletal rearrangements. Also, data showing that the electrophoretic migration of nonmyristoylated Ala-213-C-t-PAK2 is altered (Fig. 4) because of hyperphosphorylation (unpublished data) suggest that myristoylation of C-t-PAK2 might serve to localize it away from the potential inappropriate effects of some cytosolic kinase(s).

Because two of the other identified caspase-cleaved, posttranslationally myristoylated proteins are actin itself and the actin-severing protein gelsolin (12), our results indicate that posttranslational myristoylation might play a general role in the regulation of cytoskeletal structure during apoptosis. It is well known that alteration of normal cytoskeletal dynamics, such as attenuation of actomyosin cortex contractility or disruption of the structure of microtubules, can induce apoptosis. In fact, many anticancer drugs (e.g., taxol, vincristine, and vinblastine) exert their therapeutic actions by altering cytoskeletal dynamics of transformed cells (32, 33). It is possible that the changes in the cytoskeleton mediated by the deregulated C-t-PAK2 kinase activity may lead to mechanical stress that triggers cell death.

In this study, we demonstrate that membrane localization of C-t-PAK2 and its ability to induce cell death is significantly reduced when myristoylation is abolished, showing once again the importance of myristoylation in proper protein localization (10) and how this modification potentiates C-t-PAK2 function. Bisson *et al.* (28) showed that expression of an N-terminally hemagglutinin-tagged caspase-activated C-terminal *Xenopus* PAK1 (HA-C-t-xPAK1) in cells did not induce apoptosis unless a −CAAX prenylation/membrane-tethering signal was appended to it. Therefore, our results explain why this artificial membrane tethering was required; like PAK2, xPAK1, which is the functional equivalent to PAK2 (28), contains a putative myristoylation signal downstream of its caspase-cleavage site (SATDGAESSVDKTKKKPK) followed by a short polybasic domain. Importantly, with the exception of the work by Rudel *et al.* (26), all of the experiments in published articles were performed with nonphysiological forms of C-t-PAK2 bearing a variety of N-terminal epitope tags, therefore abolishing posttranslational myristoylation (16, 24, 27).

The fact that exogenous expression of C-t-PAK2 (no more than twofold; data not shown) in COS-7 cells induced striking cell retraction and nuclear condensation leading to cell death without altering mitochondrial integrity pinpoints the action of myr-C-t-PAK2 downstream of the mitochondrial commitment step and the formation of the apoptosome. In addition, it appears that the morphological changes seen in cells expressing myr-C-t-PAK2 undergoing programmed cell death do not activate the intrinsic apoptotic cell death pathway. These important observations are also supported by those of Lee *et al.* (27), Jakobi *et al.* (16), and Koeppel *et al.* (24), who showed that expression of C-t-PAK2 led to adherent cell shrinking, rounding up, and nuclear condensation without exhibiting classical hallmarks of apoptosis (no phosphatidylserine externalization and absence of TUNEL reactivity).

Because myr-C-t-PAK2-dependent events mediate cell death downstream of the mitochondrial commitment step and many cancer cells exhibit suppressed apoptosis at the mitochondrial level because of overexpression of antiapoptotic Bcl-2 family members (e.g., B cell lymphomas), finding innovative ways to activate PAK2 in cancer cells might lead to advancement in anticancer therapy.

Materials and Methods

Cell Lines, Antibodies, and Reagents. Jurkat T cells and COS-7 cells were from the American Type Culture Collection and were grown as recommended. [9,10(*n*)-^{3}H]Myristic acid and [^{125}I]NaI were from Amersham Pharmacia Biosciences. Radioiodination of the iodopalmitate [specific activity of ≈2 mCi/mmol (1 Ci = 37 GBq)] was performed as described in ref. 34. Antibodies and specialized and common reagents were from a variety of suppliers (described in *Supporting Materials and Methods*, which is published as supporting information on the PNAS web site). Plasmids were transfected into cells by using FuGENE 6 transfection reagent (Roche Applied Science, Indianapolis).

MS of Synthetic Peptides. Decapeptides (50 μM final concentration from 1 mM DMSO stocks) were incubated in NMT reaction buffer in the presence or absence of 50 μM myristoyl-CoA and 1 μg of yeast NMT. Yeast NMT was from laboratory stocks and has a wide overlapping substrate specificity with human NMTs (9). Supernatants of trichloroacetic acid precipitates were ana-

lyzed by liquid chromatography and then MS at the Institute for Biomolecular Design (University of Alberta).

Metabolic Labeling. Jurkat T and transfected COS-7 cells were metabolically labeled in their respective media without serum containing potassium [9,10(*n*)-^{3}H]myristate (400 μCi/ml or 1 mCi per 1×10^7 cells) or potassium [^{125}I]palmitate and 0.1% (wt/vol) fatty acid-free BSA for 1 h at 37°C in a humidified incubator with a 7% CO_2 atmosphere. To induce apoptosis, cells were treated for 5 h with vehicle or 2.5 μM STS and 5 μg/ml cycloheximide, a combination known to induce apoptosis in a wide variety of cells. In *N*-myristoylation inhibition studies, 1 h before metabolic labeling, medium containing 0.1% (wt/vol) fatty acid-free BSA was supplemented with 1 mM HMA (20), which was left in for the duration of the incubation.

Immunoprecipitation and Detection of Radiolabeled Proteins. Metabolically radiolabeled cells were collected and lysed in cold lysis buffer for 30 min at 4°C (11). Lysates were clarified at $1,000 \times g$ for 10 min. PAK2, myc-tagged proteins, and the various GFP constructs were immunoprecipitated with appropriate antibodies and protein G-Sepharose. Immunocomplexes were separated by SDS/PAGE (12.5%) and blotted onto PVDF membranes. PAK2 or EGFP were immunodetected by using appropriate antibodies and ECL Plus. [^{3}H]Myristate-containing PVDF membranes were washed three times in cold PBS, air-dried for 16 h, treated with EN^{3}HANCE (PerkinElmer Life Sciences), and exposed to Biomax MS film for 30–45 d at −80°C. [^{125}I]-Iodopalmitate-labeled samples were detected by using phosphorimaging (Molecular Dynamics).

Potassium Hydroxide Treatment of PVDF Membranes. PVDF membranes containing [^{3}H]myristate- or [^{125}I]iodopalmitate-labeled samples were soaked in 200 ml of either 0.2 M KOH or 1 M Tris·HCl (pH 7.0) at 25°C with shaking as described in refs. 21 and 22. Membranes were air-dried, and [^{3}H]myristate- or [^{125}I]iodopalmitate-radiolabeled proteins were detected by using the appropriate PhosphorImager screens.

Subcellular Fractionation. Transfected COS-7 cells or Jurkat T cells were fractionated into a soluble, cytosolic fraction (S) and an insoluble fraction containing mostly cellular membranes (P) as described by Berthiaume *et al.* (35). Cellular fractions were separated by SDS/PAGE (12.5%) and PAK2 was immunodetected as described above.

Live Cell Fluorescence Microscopy and Immunocytochemistry. COS-7 cells cotransfected with the various PAK2 constructs or empty vector and EGFP as a transfection marker were analyzed at 12, 16, 20, and 24 h after transfection. At each time point, cells were incubated for 15 min with 25 μg/ml permeable nuclear dye (Hoechst dye 33258; Sigma), washed twice with warm PBS, and kept in warm 0.1% FBS in PBS. Eight to 12 randomly selected fields representing 150–300 transfected cells were photographed with a Nikon epifluorescence microscope by using bright-field, FITC, and UV filters. The percentage of cells undergoing apoptosis was calculated as the percentage of green cells presenting condensed/fragmented nuclei and rounded/retracted/highly refractive morphology as described in refs. 16, 24, and 27.

Alternatively, live and fixed cell microscopy of transfected COS-7 cells was performed essentially as described in ref. 11 with the exception that 0.2% gelatin was used as a blocking agent. In colocalization studies, antibodies or fluorescent probes were used at the concentrations recommended by the suppliers (see *Supporting Materials and Methods* for details). Cells were mounted in Prolong Antifade Solution (Molecular Probes) and observed by confocal laser scanning microscopy using appropriate filter sets and excitation wavelengths.

Data Analysis. All experiments were performed three or more times. Graphs are presented as means ± SE.

We thank Drs. Michele Barry and Thomas Simmen, as well as Dale Martin, for critical reading of the manuscript. This work was supported by grants from the Cancer Research Society and the Canadian Institutes of Health Research (MOP-37955 to L.G.B.). L.G.B. is a senior scholar of the Alberta Heritage Foundation for Medical Research, which provided a Ph.D. studentship (to M.M.C.) and a summer studentship (to A.M.S.).

1. Jiang, X. & Wang, X. (2004) *Annu. Rev. Biochem.* **73,** 87–106.
2. Wyllie, A. H. (1997) *Br. Med. Bull.* **53,** 451–465.
3. Wyllie, A. H., Bellamy, C. O., Bubb, V. J., Clarke, A. R., Corbet, S., Curtis, L., Harrison, D. J., Hooper, M. L., Toft, N., Webb, S. & Bird, C. C. (1999) *Br. J. Cancer* **80,** Suppl. 1, 34–37.
4. Kerr, J. F., Wyllie, A. H. & Currie, A. R. (1972) *Br. J. Cancer* **26,** 239–257.
5. Hengartner, M. O. (2000) *Nature* **407,** 770–776.
6. Leist, M. & Jaattela, M. (2001) *Nat. Rev. Mol. Cell Biol.* **2,** 589–598.
7. Nicholson, D. W. (1999) *Cell Death Differ.* **6,** 1028–1042.
8. Zha, J., Weiler, S., Oh, K. J., Wei, M. C. & Korsmeyer, S. J. (2000) *Science* **290,** 1761–1765.
9. Farazi, T. A., Waksman, G. & Gordon, J. I. (2001) *J. Biol. Chem.* **276,** 39501–39504.
10. Resh, M. D. (2004) *Subcell. Biochem.* **37,** 217–232.
11. McCabe, J. B. & Berthiaume, L. G. (1999) *Mol. Biol. Cell* **10,** 3771–3786.
12. Utsumi, T., Sakurai, N., Nakano, K. & Ishisaka, R. (2003) *FEBS Lett.* **539,** 37–44.
13. Knaus, U. G., Morris, S., Dong, H. J., Chernoff, J. & Bokoch, G. M. (1995) *Science* **269,** 221–223.
14. Bokoch, G. M. (2003) *Annu. Rev. Biochem.* **72,** 743–781.
15. Rudel, T. & Bokoch, G. M. (1997) *Science* **276,** 1571–1574.
16. Jakobi, R., McCarthy, C. C., Koeppel, M. A. & Stringer, D. K. (2003) *J. Biol. Chem.* **278,** 38675–38685.
17. Na, S., Chuang, T. H., Cunningham, A., Turi, T. G., Hanke, J. H., Bokoch, G. M. & Danley, D. E. (1996) *J. Biol. Chem.* **271,** 11209–11213.
18. Paige, L. A., Zheng, G. Q., DeFrees, S. A., Cassady, J. M. & Geahlen, R. L. (1990) *Biochemistry* **29,** 10566–10573.
19. Galbiati, F., Guzzi, F., Magee, A. I., Milligan, G. & Parenti, M. (1996) *Biochem. J.* **313,** 717–720.
20. Nadler, M. J., Harrison, M. L., Ashendel, C. L., Cassady, J. M. & Geahlen, R. L. (1993) *Biochemistry* **32,** 9250–9255.
21. Armah, D. A. & Mensa-Wilmot, K. (1999) *J. Biol. Chem.* **274,** 5931–5938.
22. Zhao, Y., McCabe, J. B., Vance, J. & Berthiaume, L. G. (2000) *Mol. Biol. Cell* **11,** 721–734.
23. McCabe, J. B. & Berthiaume, L. G. (2001) *Mol. Biol. Cell* **12,** 3601–3617.
24. Koeppel, M. A., McCarthy, C. C., Moertl, E. & Jakobi, R. (2004) *J. Biol. Chem.* **279,** 53653–53664.
25. Jakobi, R., Moertl, E. & Koeppel, M. A. (2001) *J. Biol. Chem.* **276,** 16624–16634.
26. Rudel, T., Zenke, F. T., Chuang, T. H. & Bokoch, G. M. (1998) *J. Immunol.* **160,** 7–11.
27. Lee, N., MacDonald, H., Reinhard, C., Halenbeck, R., Roulston, A., Shi, T. & Williams, L. T. (1997) *Proc. Natl. Acad. Sci. USA* **94,** 13642–13647.
28. Bisson, N., Islam, N., Poitras, L., Jean, S., Bresnick, A. & Moss, T. (2003) *Dev. Biol.* **263,** 264–281.
29. Goto, H., Yang, B., Petersen, D., Pepper, K. A., Alfaro, P. A., Kohn, D. B. & Reynolds, C. P. (2003) *Mol. Cancer Ther.* **2,** 911–917.
30. Poot, M., Zhang, Y. Z., Kramer, J. A., Wells, K. S., Jones, L. J., Hanzel, D. K., Lugade, A. G., Singer, V. L. & Haugland, R. P. (1996) *J. Histochem. Cytochem.* **44,** 1363–1372.
31. Zhang, B., Zhang, Y. & Shacter, E. (2003) *Mol. Cell. Biol.* **23,** 5716–5725.
32. Pienta, K. J. & Coffey, D. S. (1991) *Cancer Surv.* **11,** 255–263.
33. Wang, L. G., Liu, X. M., Kreis, W. & Budman, D. R. (1999) *Cancer Chemother. Pharmacol.* **44,** 355–361.
34. Berthiaume, L., Peseckis, S. M. & Resh, M. D. (1995) *Methods Enzymol.* **250,** 454–466.
35. Berthiaume, L., Deichaite, I., Peseckis, S. & Resh, M. D. (1994) *J. Biol. Chem.* **269,** 6498–6505.